AIAA JOURNAL
Vol. 48, No. 7, July 2010

Finite Element Model Updating Using Frequency Response Function of Incomplete Strain Data

Akabr Esfandiari*
Amirkabir University of Technology, 11365 Tehran, Iran
Masoud Sanayei
Tufts University, Medford, Massachusetts, 02155
and
Firooz Bakhtiari-Nejad and Alireza Rahai
Amirkabir University of Technology, 11365 Tehran, Iran

DOI: 10.2514/1.J050039

A method is presented to detect changes in stiffness and mass parameters of a structure using strain data in the frequency domain. Sensitivity of the strain-based frequency response function is characterized as a function of the changes in stiffness, mass, and damping at the element level. The transfer function of a damaged structure is approximated using the measured natural frequencies of the damaged structure and the analytical mode shapes of the intact structure. These approximations result in a set of quasi-linear sensitivity equations. A sensitivity-based algorithm is proposed for finite element model updating. These sensitivities are used to select the measured frequency points for model updating and to investigate the weighting of sensitivity equations. The proposed method was successfully applied to a plane truss and a plane frame structure using numerically simulated, error-contaminated strain data.

Nomenclatures

A_S, A_M	=	stiffness and mass connectivity matrices
A_{Se}, A_{Me}	=	nonzero eigenvalues of element stiffness and mass matrices
B_i	=	strain-displacement mapping matrix
C	=	structural damping matrix
d	=	subscript refers to damage state
$H(\omega)$	=	transfer function matrix
I	=	index
K	=	structural stiffness matrix
L_i	=	length of the ith element
M	=	structural mass matrix
m	=	number of the measured natural frequencies
n	=	number of degrees of freedom
ne	=	number of elements
$P(\omega)$	=	vector of applied loads in frequency domain
$p(t)$	=	vectors of applied loads
P_S, P_M	=	structural stiffness and mass parameters matrices
P_{Se}, P_{Me}	=	nonzero eigenvector of element stiffness and mass matrices
$S_M(\omega, \xi)$	=	mass parameters sensitivity matrix
$S_S(\omega, \xi)$	=	stiffness parameters sensitivity matrix
T_i	=	transfer function matrix
$U(\omega)$	=	vector of displacement in frequency domain
$u(t)$	=	vectors of displacement
u_n	=	nodal displacement
$\bar{u}_n$	=	nodal displacements (local coordinates)
$\bar{x}$	=	distance from the first node of element
z	=	distance from the neutral axis
$\delta(\,)$	=	change of a variation
ε_i	=	strain of the ith element
ζ_i	=	ith damping loss factor
ξ	=	local coordinate parameter
ϕ_i	=	ith mode shape
Ω_i	=	ith natural frequency
ω	=	excitation frequency

Received 2 July 2009; revision received 19 November 2009; accepted for publication 8 December 2009.

*Also affiliated with Tufts University, Medford, Massachusetts 02155.

I. Introduction

MOST civil infrastructure, such as bridges, are in service under conditions of overestimated design loads. Many infrastructure elements have aged and deteriorated during the past few decades and are in dire need of repairs, retrofits, and possible replacements. For decision-making purposes, accurate and reliable estimations of stress distribution and deformations are needed. One way to approach this need is by using a finite element model that is calibrated with static and dynamic measurements from nondestructive tests. Such calibrated models can capture the system behavior subject to realistic loads. These precautions are paramount to guarantee robust performance of the structures, avoid further economic losses, and provide higher levels of safety.

The static and dynamic characteristics of structures, including static displacements, tilts, strains, and curvatures as well as mode shapes, natural frequencies, frequency response functions (FRFs), mode shape curvatures, modal flexibility, modal strains, and modal strain energy, are used in finite element model updating to detect, locate, and quantify structural damage [1,2].

Pandey et al. [3] and Ratcliffe [4] use modal curvature data for damage identification and state that axial and/or flexural strains (curvature) are more sensitive to localized damage within the structures, as compared with displacements. Also, strain gages are usually less expensive than accelerometers and can be embedded inside structural elements such as concrete dams or concrete bridge decks to measure the response of inaccessible parts of structures. However, careful attention to strain gage installation is necessary to avoid adverse effects of local stress and concrete cracking. Preparing instrumentation setup for full-scale structures using strain gages is easier than using static displacement transducers because strain gages are reference independent.

Axial or flexural strain data can be used either in the static or dynamic state. Sanayei and Saletnik [5] developed a sensitivity-based method of parameter estimation using a subset of the static strain data. Residuals of predicted and measured strains were minimized with respect to element stiffness parameters. The

proposed method was verified using experimental data from a two-story frame using static strains and displacements [6]. Liu [7] used static strain measurements to identify the stiffness of a frame. Liu and Chian [8] developed a method for identifying the element properties of a truss using axial strains by minimizing the error norm of the equilibrium equation. They studied identifiability of structures using the inverse problem in the presence of measurement errors. Shenton and Xiaofeng [9] proposed a static strain-based method for damage identification in civil structures based on the idea that dead load is redistributed when damage occurs in the structure. The inverse problem is defined by a constrained optimization problem and is solved using a genetic algorithm. Results show that damage is difficult to identify when it is close to the inflection point of an undamaged beam, where the dead load strain is zero.

Pandey et al. [3] and Ratcliffe [4] state that strain (axial or flexural) is more sensitive to observing changes in unknown parameters for damage identification in comparison to using displacement measurements. For static loading, this statement only holds for indeterminate structures and does not apply to determinate structures. For determinate structures, strains are a function of the internal moments and forces, which are independent of material and section properties. As a result, strain measurements cannot observe changes of elements stiffness in determinate structures. For indeterminate structures, changes in static displacements and strains are a function of the system stiffness, since changes in the stiffness of one element redistribute stresses in all elements. This phenomenon increases the chance of observing structural damage due to indeterminacy.

Static methods can identify only stiffness parameters and are not able to capture any changes in mass and damping parameters, while dynamic methods can identify changes in all structural parameters. Hence, some researchers are interested in updating structural models using dynamic methods via natural frequencies, mode shapes, mode shapes curvatures, and FRF data. Pandey et al. [3] showed how damage causes change in the curvature of the mode shape, which can be used to detect the location of cracks by comparing the curvature of the mode shapes of damaged and undamaged structures. Mode-shape curvatures were extracted from displacement mode shapes. The curvature mode shape information was used by Pabst and Hagedorn [10] in combination with changes in measured frequencies. Salawu and Williams [11] compared the performance of both the curvature and the displacement mode shapes for locating damage. They point out that the most important factor is the selection of mode shapes for analysis. Stubbs and Kim [12] used curvature modes as a damage index. Wahab and Roeck [13] employed a mode curvature damage factor for modal updating, and Shi et al. [14] introduced the ratio of change in modal strain energy in each element as another damage indicator. Lestari and Qiao [15] proposed an approach using the curvature mode shapes to detect debonding and core crushing in composite honeycomb sandwich beams, and both the location and the extent of damage were evaluated.

One of the challenges in finite element model updating is the number of measured data points compared with the number of unknown structural parameters. The number of measured data points adopted can restrict the capability and stability of parameter estimation methods. Damage detection using measured FRF is an alternative to dealing with limited data and has been studied by a number of researchers [16–18]. Using direct FRF measurements has several advantages. FRF-based parameter estimation methods can provide an abundance of information at a large number of frequencies, using measured data at selected degrees of freedom (DOFs) and desired frequency ranges, as opposed to modal data, which are extracted from a very limited number of the FRF data only at resonance frequencies. Additionally, FRF data can be extracted without further numerical processing and hence will not be contaminated by modal extraction errors and loss of information due to curve fitting. FRF data measured near resonances are less accurate when compared with data measured away from resonances. As a result, mode shapes extracted from FRFs can contain large errors. Because of the inaccuracies in extracted mode shapes and limited data points at resonances, it is more reliable and practical to directly use measured FRF data for finite element model updating.

Keilers and Chang [19] used frequency domain data and the mode shape curvature for parameter estimation. They investigated the use of piezoelectric sensors built into laminated composite structures to detect delamination and estimate its location and size. Sampaio et al. [20] and Schulz et al. [21] used FRF information. These FRF-based curvature methods performed well in detecting and locating the damage, especially for large magnitudes of damage. Colin and Ratcliffe [22] used measured FRFs to obtain displacement as a function of frequency and convert it to curvature functions, which was further processed to yield a damage index. Results showed the proposed method is highly sensitive to damage, and can locate and quantify even a small change.

Although the number of data points can be larger than the number of unknowns, for both static and dynamic response algorithms the number of transducers is far less than the number of DOFs in the finite element model. Hence, it is essential that the stiffness and mass matrices be reduced or the measured response data be expanded to estimate required data at unmeasured locations [23–25]. Sazonov and Klinkhachorn [26] discussed the application of a model-based approach to locating damage with all deflection data. These data should be expanded from the measured deflection response using curvature and strain mode shapes. A cantilever steel beam damaged in one location and a cantilever beam with damage in multiple locations were tested, and the effectiveness of the proposed method was verified by a comparison with the experimental results.

In this paper, a finite element model updating technique is presented using strain data in the frequency domain. Strain-based FRFs are used to correlate changes of axial or flexural strain to changes of stiffness, mass, and damping of structures. To remove the drawback of incomplete measurements in derivation of the sensitivity equation, the transfer function of the damaged structure is approximated using the measured natural frequencies and modal damping loss factors of the damaged structure. Quasi-linear sensitivity equations are solved for finite element model updating by the least square method (LS) in a few iterations. The effects of weighting methods for improving accuracy of parameter estimates are studied. Additionally, a sensitivity-based criterion is used for the selection of frequency ranges for robust optimization. Noise-contaminated FRF data of a truss and a frame model are used to verify the proposed method. These examples show successful structural parameter estimation for damage assessment.

II. Strain-Based Transfer Functions for Parameter Estimation

A similar derivation of strain-displacement relations by Sanayei and Saletnik [5] is used in this research using dynamic strain data. A two-dimensional frame element representing axial and bending deformations is shown in Fig. 1. The relationship between nodal displacements $\bar{u}_i$ and element strains ε_i is defined as

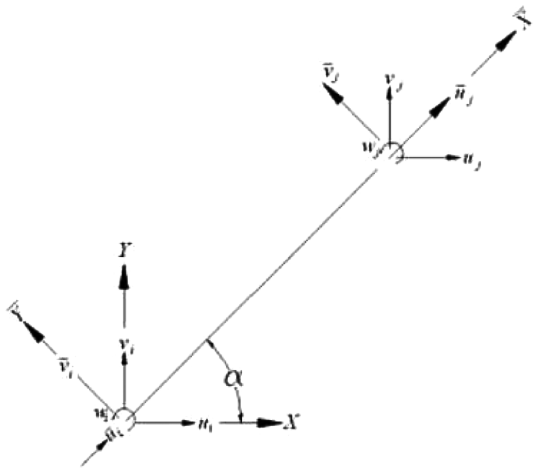

Fig. 1 A one dimensional element in a two-dimensional space (truss or beam element).

$$\varepsilon_i = B_i \bar{u}_i \tag{1}$$

Where $\bar{u}_i$ is represented in the local coordinates $(\bar{X}, \bar{Y})$. The strain-displacement mapping matrix is defined as B_i for axial and bending deformations. For an axial element, B_i is defined as

$$B_i = \frac{1}{L_i}[-1 \quad 0 \quad 1 \quad 0] \tag{2}$$

L_i is the length of the ith element. For a beam-column element

$$B_i = \left[\frac{-1}{L_i} \quad \frac{-6z\xi}{L_i^2} \quad \frac{-z(6\xi-2)}{2L_i} \quad \frac{1}{L_i} \quad \frac{+6z\xi}{L_i^2} \quad \frac{-z(6\xi+2)}{2L_i}\right] \tag{3}$$

z is the distance from the neutral axis of the beam cross-section, ξ is the local coordinate parameters as

$$\xi = 2\bar{x}/L_i - 1 \tag{4}$$

and $\bar{x}$ is the distance from the first node in the local coordinates. By assembling Eq. (4) for all ne elements and in the global coordinates, the strain-displacement relation for whole structural elements will be expressed as

$$\varepsilon(\xi) = \sum_{i=1}^{ne} B_i(\xi) T_i \bar{u}_i = B(\xi) u \tag{5}$$

T_i is the transformation matrix that maps nodal displacement from the global coordinates to the local coordinates. The vector of the measured nodal displacements, u_i, in the global coordinate system should be extracted from the vector of the displacements for static loads or dynamic excitation.

The dynamic equation of motion for an n DOF structure in the global coordinate system is

$$M\ddot{u}(t) + C\dot{u}(t) + Ku(t) = p(t) \tag{6}$$

where M, C, and K are $n \times n$ matrices of mass, damping, and stiffness, respectively, and $p(t)$ and $u(t)$ are $n \times 1$ vectors of applied loads and displacements, respectively. Also, dot superscripts indicate derivations with respect to time. Applied load and displacement response can be represented as

$$p(t) = P(\omega)e^{j\omega t} \tag{7a}$$

$$u(t) = U(\omega)e^{j\omega t} \tag{7b}$$

Substituting Eqs. (7a) and (7b) in Eq. (6) yields

$$(-\omega^2 M + j\omega C + K)U(\omega) = P(\omega) \tag{8}$$

Defining transfer function matrix $H(\omega)$ as

$$H(\omega) = (-\omega^2 M + j\omega C + K)^{-1} \tag{9}$$

Equation (8) is rewritten as

$$U(\omega) = H(\omega)P(\omega) \tag{10}$$

In a damaged state, Eq. (10) can be expressed as

$$U_d(\omega) = U(\omega) + \delta U(\omega) = H_d(\omega)P(\omega) \tag{11}$$

where

$$H_d(\omega) = [(-\omega^2(M + \delta M) + j\omega(C + \delta C) + (K + \delta K)]^{-1} \tag{12}$$

Expanding Eq. (11) and subtracting Eq. (10) from it yields

$$\delta U(\omega) = H_d(\omega)(-\omega^2 \delta M + j\omega \delta C + \delta K)U(\omega) \tag{13}$$

In Eq. (13), $\delta U(\omega)$ of size $(n \times 1)$ represents the residual between the analytical and measured FRFs at each measured DOF. It is a linear function of δM, δC, and δK. System displacement spectrum $U(\omega)$ of size $(n \times 1)$ is calculated analytically for the structural system. By substituting Eq. (13) in Eq. (5), strain-based damage-induced changes in the frequency domain are evaluated as

$$\delta\varepsilon(\omega, \xi) = H_{\varepsilon d}(\omega, \xi)(-\omega^2 \delta M + j\omega \delta C + \delta K)U(\omega) \tag{14}$$

where strain-based transfer function is

$$H_{\varepsilon d}(\omega, \xi) = B(\xi)H_d(\omega) \tag{15}$$

In Eq. (14), $\delta\varepsilon(\omega, \xi)$ of size $(ne \times 1)$ represents the residual between the analytical and measured strain spectrums at each strain gage. This formulation can accommodate several strain measurements per element at any depth of the member, if desired. Using directly measured $H_{\varepsilon d}(\omega, \xi)$ or computing it by using measured $H_d(\omega, \xi)$, Eq. (14) represents exact linear sensitivity of the structural response with respect to the change of structural parameters. Using Eq. (14), one is able to estimate change in structural parameters without any iterative process. It is impossible to use such a sensitivity equation in real applications, due to lack of a complete set of data. For large existing structures, instrumentation at all DOFs is costly, and internal DOFs are not accessible.

In this study an accurate approximation of $H_d(\omega, \xi)$ is proposed to deal with the impossibility of its measurement. The transfer function matrix in Eq. (12) can be expressed using the modal coordinate decomposition $H(\omega)$ as

$$H(\omega) = \sum_{i=1}^{n} \frac{\phi_i \phi_i^T}{\Omega_i^2 - \omega^2 + 2j\zeta_i \Omega_i \omega} \tag{16}$$

ϕ_i, Ω_i and ζ_i are the ith mode shapes, natural frequency, and damping loss factor of the intact structure, respectively. Also, one can use a truncated form of Eq. (16) to compute transfer function in the decomposed form using mode shapes and natural frequencies. It is desirable to keep the benefits of using a linear set of sensitivity equations ensuring robustness and fast convergence. For this purpose, the transfer function is evaluated in the decomposed form using analytical mode shapes of the intact structure and incomplete measured natural frequencies and damping loss factors of the damaged structure. The proposed evaluation of $H_d(\omega)$ is shown as

$$H_d(\omega) \cong \sum_{i=1}^{m} \frac{\phi_i \phi_i^T}{\Omega_{id}^2 - \omega^2 + 2j\zeta_{id}\Omega_{id}\omega} + \sum_{i=m+1}^{n} \frac{\phi_i \phi_i^T}{\Omega_i^2 - \omega^2 + 2j\zeta_i \Omega_i \omega} \tag{17}$$

where m is the number of the measured natural frequencies and Ω_{id} and ζ_{id} are the ith measured natural frequency and damping loss factor of the damaged structure, respectively. The second part in Eq. (17) is added to increase its accuracy by reducing the effects of the incomplete measurements in the decomposed form of the transfer function. This second part of Eq. (17) corrects itself as the optimization process updates the parameters of the structure.

It is necessary to emphasize that as an alternative to dealing with incomplete measurements, unmeasured DOFs can be condensed out from finite element models [23–25]. Condensing out will convert the linear sensitivity Eq. (14) to an algebraically nonlinear set of equations. The solution of a nonlinear set of equations by an iterative method is numerically not as stable as that of a linear set of equations. There is also no major difference between deriving the sensitivity equation by a condensation method and doing so by differentiating the transfer function of the structure with respect to the unknown stiffness and mass parameters. To remove the drawback of incomplete measurements, one can use a data expansion method such as techniques used in the mode shape-based methods. It is evident that although the sensitivity equation will remain linear, data expansion will introduce more errors in data and results in less accurate parameter estimates.

The stiffness and mass matrices of axial or bending elements can be described as follows [27]:

$$K_e = A_{Se} P_{Se} A_{Se}^T \tag{18a}$$

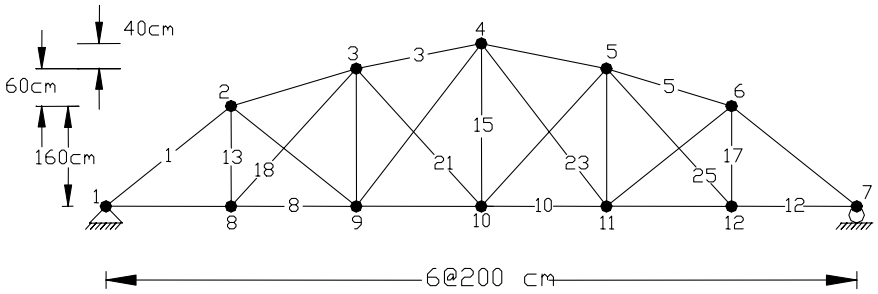

Fig. 2 Bowstring truss structure.

$$M_e = A_{Me} P_{Me} A_{Me}^T \tag{18b}$$

where A_{Se} and A_{Me} contain corresponding eigenvectors of nonzero eigenvalue of the stiffness and mass matrices of each element, P_{Se} and P_{Me} contain nonzero eigenvalue of stiffness and mass matrices as their diagonal entries. The stiffness and mass matrices of the structure are constructed by assembling the elemental stiffness and mass matrices as

$$K = \sum_{i=1}^{ne} T_i^T A_{Sei} P_{Sei} A_{Sei}^T T_i = A_S P_S A_S^T \tag{19a}$$

$$M = \sum_{i=1}^{ne} T_i^T A_{Mei} P_{Mei} A_{Mei}^T T_i = A_M P_M A_M^T \tag{19b}$$

The number of elements of the structural system is ne. Matrices A_S and A_M are defined as the stiffness and mass connectivity matrices, and the diagonal matrices of P_S and P_M has the elemental stiffness and mass parameters as their diagonal entries. Examples of the stiffness-related parameters are axial and flexural rigidities, and examples of mass parameters are mass per unit length. The number of parameters is dependent on the number of elements and their types.

Since the global stiffness matrix is a linear function of elemental stiffness and mass parameters and A_s and A_M are independent of P_s and P_M, Eq. (19) can be perturbed to get

$$K + \delta K = A_S (P_S + \delta P_S) A_S^T \tag{20a}$$

$$M + \delta M = A_M (P_M + \delta P_M) A_M^T \tag{20b}$$

where δP_S and δP_M are the changes of elemental stiffness and mass parameters caused by damage. Expanding Eq. (20) and subtracting Eq. (19) from it yields a parameterized form of the perturbed global stiffness and mass matrices as

$$\delta K = A_S \delta P_S A_S^T \tag{21a}$$

$$\delta M = A_M \delta P_M A_M^T \tag{21b}$$

Substituting Eq. (21) in Eq. (14), change of the element's strain can be correlated to the changes in stiffness and mass parameters as

$$\delta\varepsilon(\omega, \xi) = S_S(\omega, \xi)\delta\bar{P}_S + S_M(\omega, \xi)\delta\bar{P}_M \tag{22}$$

$$S_S(\omega, \xi) = H_{\varepsilon d}(\omega, \xi) A_S \mathrm{diag}(A_S X(\omega)) \tag{23}$$

and

$$S_M(\omega, \xi) = -\omega^2 H_{\varepsilon d}(\omega, \xi) A_M \mathrm{diag}(A_M X(\omega)) \tag{24}$$

$\delta\bar{P}_S$ and $\delta\bar{P}_M$ are vectors of changes in stiffness and mass parameters, respectively, and function diag represents entries of a vector as a diagonal matrix. To estimate changes in stiffness and mass properties, sensitivity Eq. (22) can be solved by several methods such as the LS, nonnegative least square method, or singular value decomposition method. For a reliable and high-confidence solution, several factors should be addressed, including the sensor types and locations, excitation types and locations, quality of measured FRF data (measurement error), accuracy of the mathematical model (modeling error), observability of the unknown parameters, sensitivity equation weighting, and numerical methods used to solve the equations set. In solving Eq. (22) for the unknown parameters, a balanced attention to the above factors is expected to result in an error-tolerant and robust parameter estimation system for finite element model updating.

Several methods have been suggested in the literature for weighting the system of equations. Each equation can be normalized by its second norm so all equations have the same weight in parameter estimation. Equations with smaller sensitivities to the unknown parameters should be removed prior to normalization [28], since these equations have low observability of the unknown parameters and can cause ill-conditioning. In Eq. (22), if the ith equation associated with frequency ω has elements $\varepsilon(\xi, \omega)$ and $\varepsilon_d(\xi, \omega)$ of similar magnitudes, the adverse effects of measurement errors may be significantly magnified after the weighting. To overcome this problem, such an equation should be removed [28]. Statistical methods are also available for weighting sensitivity equations based on the accuracy of measurements. In this research, each row of the sensitivity matrix is normalized by its norm to have a robust parameter estimation system. Also, equations with small sensitivity are avoided by the appropriate selection of the excitation frequencies.

III. Truss Example

A two-dimensional truss, as shown in Fig. 2, is used to investigate robustness of the proposed finite element model updating method. The unknown parameters used for model updating are axial rigidity of elements EA, which is the cross-sectional area of elements multiplied by Young's modulus. Cross-sectional areas of truss members are given in Table 1.

For the bowstring truss with 21 DOFs in Fig. 2, the FRF data can be extracted from an experimental nondestructive test. Here, representative FRFs were simulated using the finite element method. A single harmonic load is applied at the DOFs number 4, 13, and 19 as three independent load cases. Elements number 8, 11, 13, 14, 15 and 23 are selected for measuring strains since these are pure axial elements and strains are constant along each member.

IV. Challenges and Solutions in Using Frequency Response Function Data for Parameter Estimation

In finite element model updating using experimental data, there are unavoidable errors due to the presence of modeling errors and measurement errors. Modeling errors are beyond the scope of this research. Although it might be impossible to capture various types of measurement errors using numerical simulations, measurement

Table 1 Cross-sectional area of truss members

Member	Area, cm^2
1–6	18
7–12	15
13–17	10
18–25	12

errors are simulated by adding a series of random values to the theoretically calculated responses. In this study, a 10-percent uniformly distributed random noise is proportionally added to the calculated strains of the FE model.

FRFs of the bowstring truss will be used for parameter estimation using Eq. (22). As a part of this estimation, measured natural frequencies are used in the calculation of transfer functions Eq. (17). Some researchers assume that the natural frequencies of lightly damped structures can be measured nearly noise-free or at least with a high level of confidence using available precise, low-noise accelerometers and data acquisition systems [29]. Numerical simulation by the authors shows that adding 0.5-percent normally distributed random noise to the measured natural frequencies does not significantly impact the estimated parameters if the excitation frequency is not in the vicinity of the nearest measured natural frequencies. In this study, therefore, all simulations of the damaged truss are considered noise-free. It is also assumed that the first ten natural frequencies of the damaged truss are measurable for all load cases.

Generally, the success of a FRF-based model updating process is dependent on selection of the frequency points, quality of measurements, and capability of the algorithm (sensitivity equation) to capture real behavior of the structure. Understanding the approximations made in Eq. (17) and its impacts on the behavior of FRFs is paramount in the proposed method. The behavior of the approximate solution and the selection of frequency ranges are discussed using the next four figures. For illustration purposes, samples of lightly damped and highly damped transfer functions of intact and damaged structures are graphed in Fig. 3.

A FRF-based model updating technique attempts to minimize the residual between the FRFs of the intact and damaged structures. Hence, in an iterative model updating technique, the FRF of the intact structure (analytical) should move toward the FRF of the damaged structure (measured). Figure 3 shows by vertical lines that there are two possible positions for residuals of FRFs. These residuals can be related to a frequency point between the resonances of the intact and damaged structure (region 1) or may be related to frequency points out of this interval (region 2). A decrease of these residuals during the iteration process is expected. The residual at a frequency point to the right side of region 1 increases at the primary iteration of model updating and then decreases. Frequency points to the left side of region 1 tend towards the opposite direction. It should be noted that the widths of the defined regions change during the optimization process, which converts model updating to a nonsmooth and monotonous optimization, which is not desired. For a frequency point in region 2, residuals decrease as the model updating converges. Only regions that residuals reduce monotonically should be used in the optimization process. Therefore, region 1 should not be used.

Since a perfect match of the FRFs of the damaged and intact structures is not always possible, some nonsmooth behavior will occur at points close to the resonance frequencies. These points should therefore be excluded from the frequency points for model updating.

Some model updating methods assume zero damping ratios. For lightly damped structures, this assumption does not have a major effect on the result of model updating that uses modal data. As Fig. 3 shows, the damping loss factor is important at frequencies close to responses, and controls the amplitude of FRFs. Damping effects decrease rapidly by moving frequency points away from the resonances. It is therefore necessary to be aware of damping effects in model updating. Damping can be modeled by various methods, including Modal, Rayleigh, and Coulomb. These methods, however, might not be able to represent damping effects for a real structure, especially around resonances. Therefore, in this paper, frequency points are selected at regions far enough away from resonances not to consider damping for model updating. If damping is included in model updating, by moving the excitation frequency away from the resonance frequency, response is less sensitive to the shortcomings of using damping in the analytical model and to errors in damping measurements.

Selected excitation frequency points must not be very close to the natural frequencies of the damaged structures in order to prevent noisy measurements due to resonance phenomena. For low modal damping ratios, capturing accurate measurements at resonance is challenging due to sharpness of response. Based on the sampling rate used, the peak resonance can be truncated. In addition, in higher frequency ranges, the response of a structure is more local, and therefore more sensitive to damage, compared with the response in low frequency ranges. Therefore, it is expected that higher excitation frequencies, which excite the higher mode shapes, yield better results.

The only approximated term in the derivation of the sensitivity Eq. (22) is the transfer function of the damaged structure evaluated by Eq. (17). Therefore, confidence of the estimated parameters depends heavily on how this equation represents the transfer function of a damaged structure. Equation (17) is approximate since

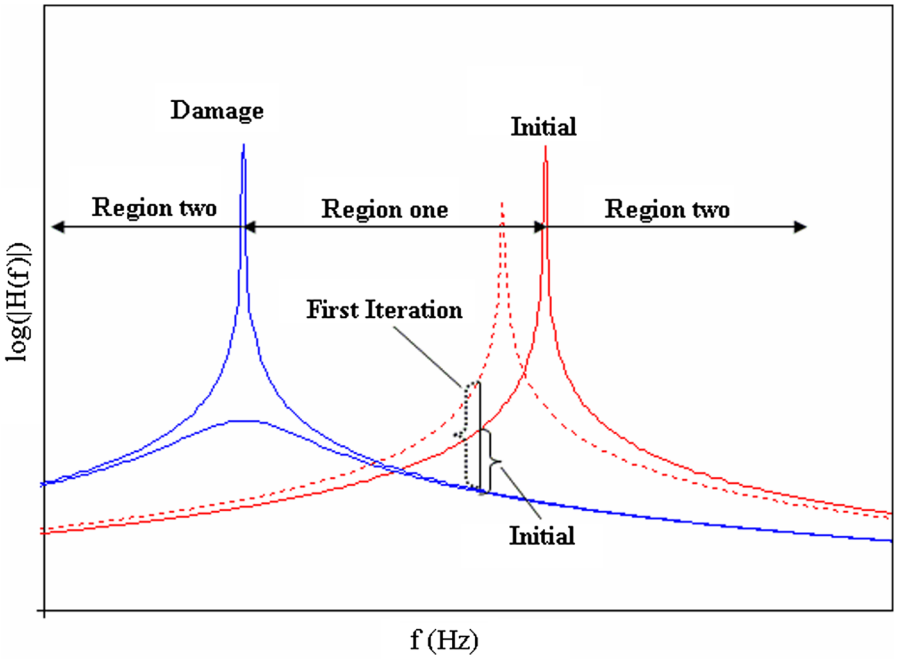

Fig. 3 FRF of an intact and related damaged structure with different damping ratios.

an incomplete set of measured natural frequencies is used, and mode shapes of the intact structure are used instead of mode shapes of the damaged structure. These two types of approximations are investigated here and shown in Figs. 4–6.

The first source of approximation in Eq. (17) is using an incomplete set of measured natural frequencies. The FRF of an arbitrary point in the truss structure is plotted in Fig. 4. These FRFs are evaluated using 8, 10, 15, and 21 (exact) analytical mode shapes and natural frequencies.

As Fig. 4 illustrates, the number of required natural frequencies and mode shapes is dependent on the excitation frequencies. Although estimating FRF using a truncated set is very accurate for frequencies at low ranges, accuracy decreases as the frequency increases. However, this approximation is still valid in the vicinity of all resonance frequencies, since in these regions amplitude of the FRF is controlled by the nearest resonance in the denominator of Eq. (17). Figure 4 shows that the approximate transfer function evaluated by Eq. (17) using the ten first natural frequencies is accurate in the vicinity of resonances up to 367.5 Hz and completely failed after this point (10th resonance is 367.5 Hz). The same is observed by evaluating the FRF using other numbers of incomplete modal data. This indicates that the approximation of transfer function by Eq. (17) is valid in the ranges of the measured natural frequencies.

The second source of approximation in Eq. (17) is using the mode shapes of the intact structure instead of the mode shapes of the damaged structure. To study the effects of this assumption, a sample FRF using 10 and 15 first mode shapes of the intact structure and natural frequencies of the damaged structure along with the exact FRF are graphed in logarithmic scale in Fig. 5.

As Fig. 5 illustrates, the effect of using intact mode shapes is small in the low frequency ranges. For high frequency ranges, this replacement is not too important because frequency points in the vicinity of resonance frequencies and approximation are still valid. This is true in the higher frequency ranges due to the fact that the amplitudes of FRFs are controlled by the denominator of Eq. (17).

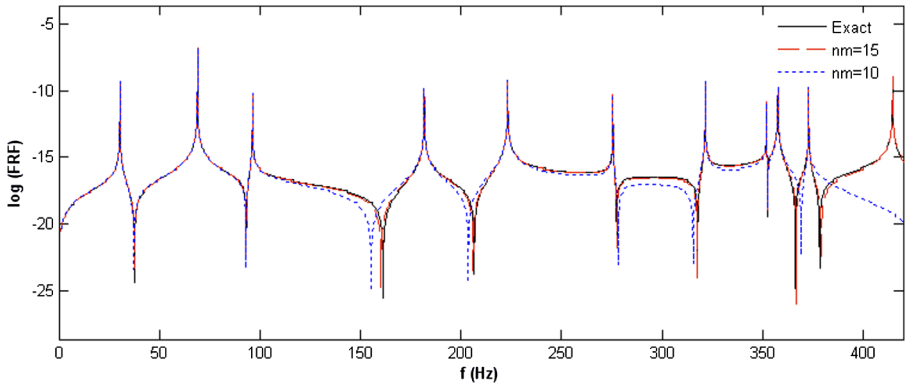

Fig. 4 Exact and approximate FRFs using incomplete sets of measured modes of vibrations in Eq. (17).

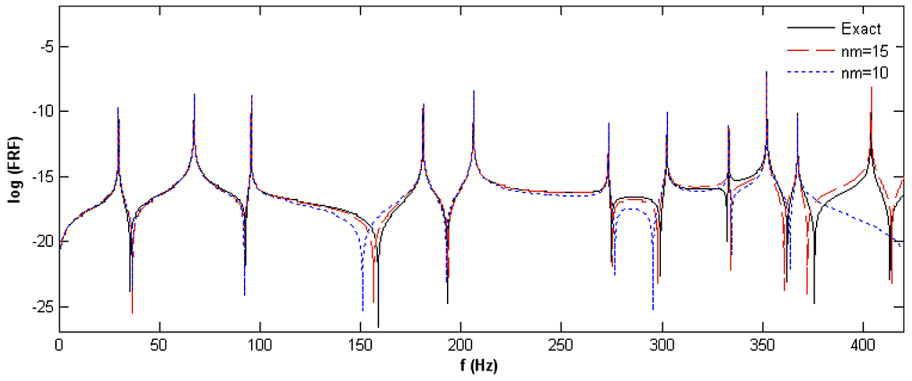

Fig. 5 Exact and approximate FRFs using mode shapes of the intact structure in Eq. (17).

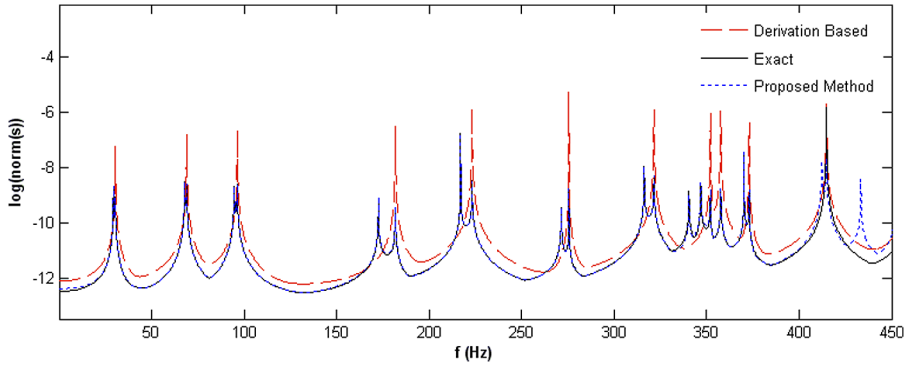

Fig. 6 Norm of the sensitivity equation for a single excitation at DOF no. 11.

The success of a model updating technique is dependent on the derivation of the sensitivity matrix and selection of frequency ranges for model updating. The derivation of an accurate linear sensitivity equation such as Eq. (14) is desirable for parameter estimation. However, such a sensitivity equation is impractical since it needs full instrumentation at all DOFs. As stated before, options for dealing with incomplete measurements using sensitivity-based model updating algorithms are data expansion, model reduction, or use of derivation-based sensitivity equations, which have their shortcomings. Derivation of an inverse matrix such as transfer function $H(\omega)$ or $H_\varepsilon(\omega, \xi)$ is commonly evaluated as [30]

$$S(\omega, \xi) = [\, S_S \quad S_M \,] = \left[H_\varepsilon(\omega, \xi) \tfrac{\partial K}{\partial P_S} U(\omega)) \quad -\omega^2 H_\varepsilon(\omega, \xi) \tfrac{\partial M}{\partial P_M} U(\omega)) \right] \tag{25}$$

This sensitivity equation needs to be calculated in each iteration and may represent nonsmooth behavior during optimization and is not used in this paper. By using the proposed approximation for $H_d(\omega)$ in Eq. (17), this study proposes a quasi-linear sensitivity equation that yields a robust model updating technique. At the selected frequency points, the response of the structure should be sensitive to change in structural parameters for target elements. In model updating, sensitivity is a function of the locations of measurements, excitations, frequency ranges, and topology of the structure. Studies on sensor placement and selection of excitation locations lead to a combinatorial optimization problem that is out of the scope of this paper. Given a set of sensor locations and excitation points, for parameter estimations, it is desirable to have the highest value of change in the response (sensitivity) due to changes in the unknown structural parameters. For a specific excitation point, the norm of the sensitivity matrix can be considered as a scale to adopt the best points of excitation. In Fig. 6 the second norm of the sensitivity matrix for damage case 2 is plotted in a logarithmic scale as a function of frequency.

Large differences between norms of the sensitivity equation of a derivation-based method in Eq. (25) and the exact one in Eq. (14) indicate large differences in the entries of these two sensitivity matrices. These differences can cause divergence of the optimization process in the presence of measurement errors. Regardless of values of the norm of the sensitivity matrix, Fig. 6 shows that a derivation-based sensitivity equation doses not represent the real behavior of the changes in FRFs. In Fig. 6, for example, the large norm of the exact sensitivity equation indicates that the best sensitivities are near the resonance frequencies of the intact and damaged structures while a derivation-based sensitivity equation shows a good sensitivity around the resonance of the intact structure. Therefore, using a derivation-based sensitivity can result in missing the best frequency points of FRFs for model updating. It should be noted that a good match between norm values of the proposed approximate sensitivity matrix by Eq. (22) and analytical exact sensitivity matrix by Eq. (14) does not mean that the proposed approximate matrix is as accurate as an exact one, however, only a few iterations are still necessary for model updating. This is an indication of robustness and quasi linearity of this method.

All of the measured FRFs should not be used for finite element model updating. Although Fig. 6 shows that the best points for model updating are close to the resonance frequencies of the intact and damaged structures, frequency points very close to resonances and also between them should be excluded to avoid nonsmooth behavior in the optimization process. In consideration of these limitations, an interval of 5 Hz around the resonances is excluded from model updating. Also, as Fig. 6 shows, the maximum norm of the sensitivity equation occurs around resonances and decreases rapidly as it moves away from resonances. To avoid low sensitivity frequency points, in this study, excitation frequency ranges are selected at the regions in which the norm of the sensitivity equation is higher than 5% of the maximum norm of the sensitivity matrix around resonances. Frequency points are selected at 1 Hz intervals.

V. Model Updating for Damage Detection Using Truss Example

For the truss example, six damage cases are considered to investigate robustness of the proposed parameter estimation method in locating and quantifying damage. Bar charts indicate location and severity of the damage by black bars and indicate predicted results by white bars. Selected frequency ranges used in model updating are given in Table 2.

To investigate the reliability of the method, 50 sets of random noise-contaminated data are considered. To show robustness and confidence of the predicted parameters, averages of the estimated parameters are plotted in Figs. 7–12 along with the coefficient of variation (COV) of the predicted parameters, standard deviation divided by average. Low COV of the predicted parameters indicates as a low scattering in the predicted parameters. COV values corresponding to the damaged elements are shown by black bars.

Figures 7–12 show the possibility of detecting the severity and location of damage using the proposed method. For most of the estimated parameters, COV are less than 5%, indicative of very robust and low-scatter prediction results. Also, the very low COV value of the damaged elements shows these elements identified with a high level of accuracy and confidence. A comparison of Figs. 11 and 12 shows a lower confidence level of mass parameters prediction in comparison with the stiffness prediction. This indicates a lower observability of mass parameters at selected frequency ranges, which can be improved by using higher frequency ranges.

VI. Model Updating for Damage Detection Using Frame Example

A one-story one-bay aluminum frame, as shown in Fig. 13, is considered to verify the damage identification method described in this paper. The finite element analysis is carried out to simulate the experimental data by using two-node frame elements. The number of nodes and elements are 22 and 21, respectively. The length of each element is 10 cm with cross-section areas of 3.6 cm^2 and moment of inertia of 0.2644 cm^4. The unknown parameters of the elements are flexural rigidity, *EI*, and axial rigidity, *EA*.

A strain gage measured a strain value that consists of both axial and flexural strains. It is therefore necessary that both axial and flexural rigidities be considered in model updating. Exciting a structure in axial mode is difficult in reality, leading to failure of parameter estimation because of low contribution of axial rigidity to the sensitivity matrix of FRFs. Although in this paper only flexural rigidities are updated, data of the damaged structure are simulated by considering changes of both axial and flexural rigidities of the damaged elements.

Based on the previously discussed points and limitations, frequency points for model updating are adopted as given by Table 3. Element numbers 2, 6, 9, 13, 16, and 19 are considered to measure strains. Unit harmonic loads are applied at node numbers 4, 7, 12, 17, and 19, perpendicular to the structure.

In mass identification cases, the sensitivity equation was ill-conditioned, since sensitivities of elements 1 and 21 were very small compared with other elements, causing a failure of model updating even using noise-free data. Therefore, the parameters of these two elements are assumed to be known and have not been updated. Predicted damage and COV of the predicted parameters are given in Figs. 14–19.

Table 2 Selected frequency ranges for truss model updating

Damage case: 1, 2	Damage case: 3, 4	Damage case: 5, 6
190–210	190–205	185–205
225–235	235–255	225–245
280–285	285–295	280–290
325–335	330–340	325–340
360–365	370–380	375–385

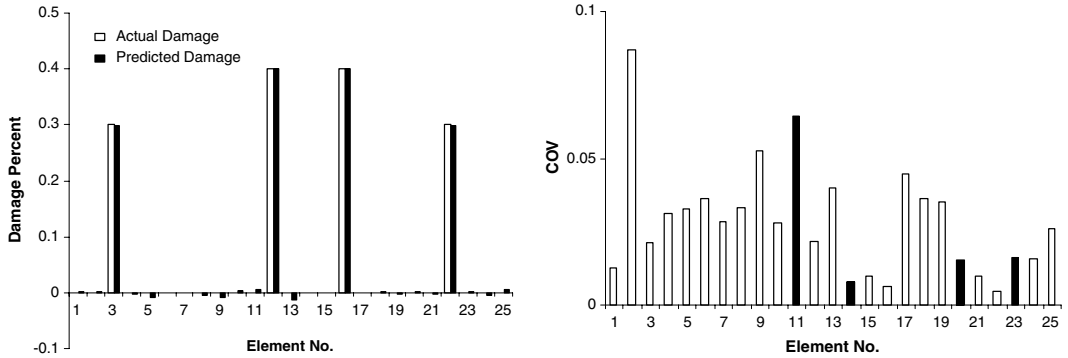

a) b)

Fig. 7 a) Actual and predicted truss stiffness change for case 1 and b) COV of predicted parameters.

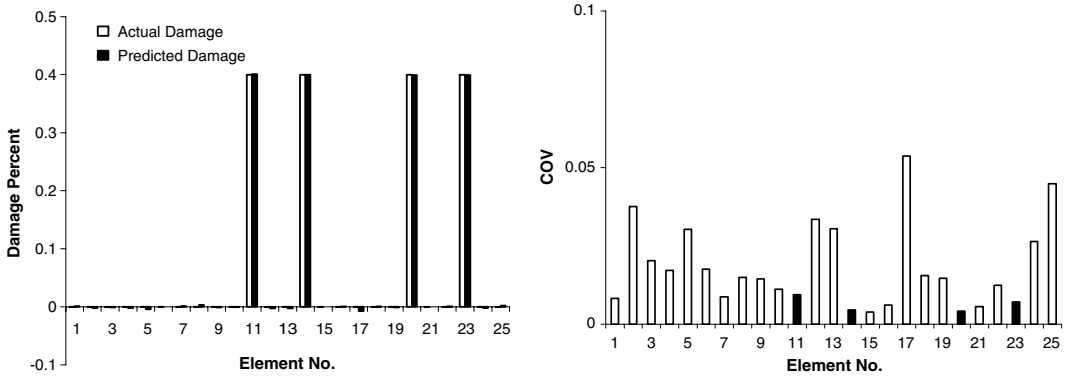

a) b)

Fig. 8 a) Actual and predicted truss stiffness change for case 2 and b) COV of predicted parameters.

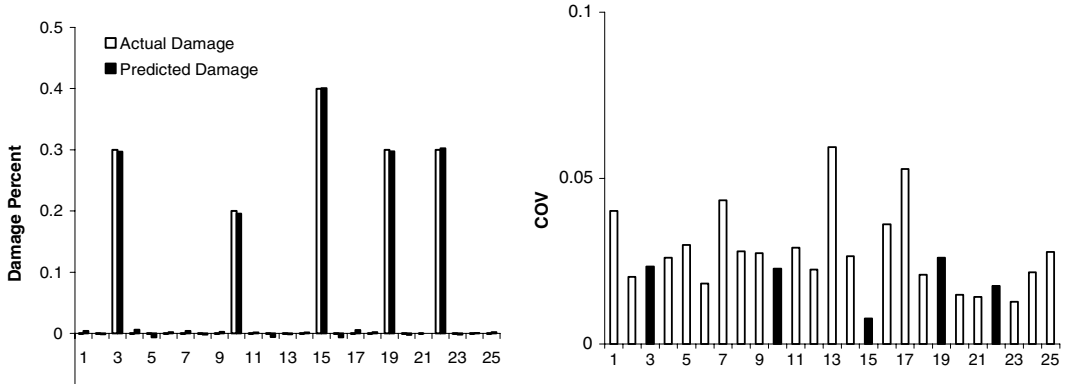

a) b)

Fig. 9 a) Actual and predicted truss mass change for case 3 and b) COV of predicted parameters.

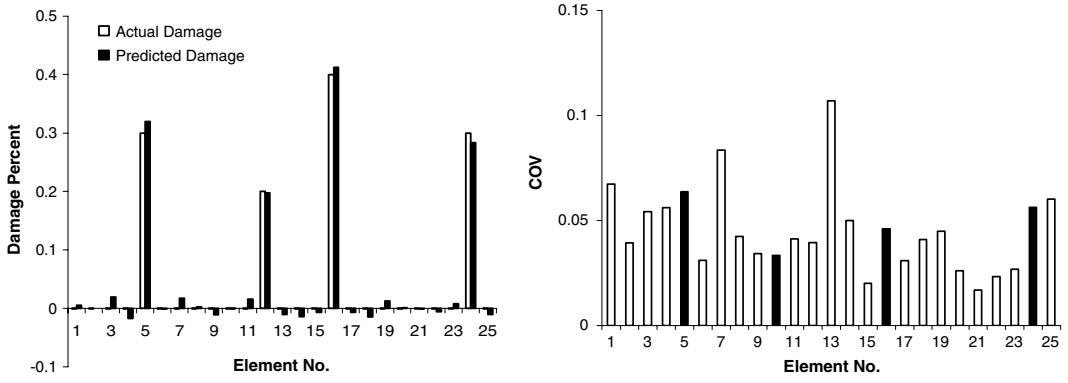

a) b)

Fig. 10 a) Actual and predicted truss mass change for case 4 and b) COV of predicted parameters.

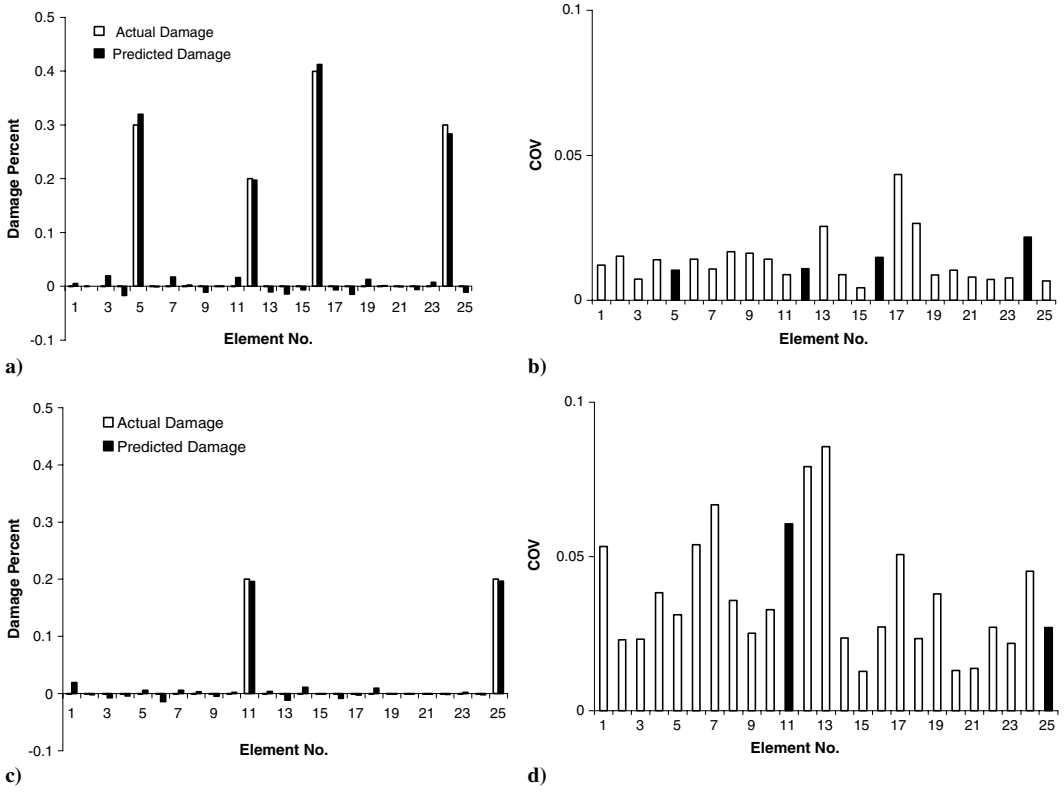

Fig. 11 a) Predicted truss stiffness change in case 5, b) COV of predicted stiffness parameters, c) predicted truss mass change for case 5, and d) COV of predicted mass parameters.

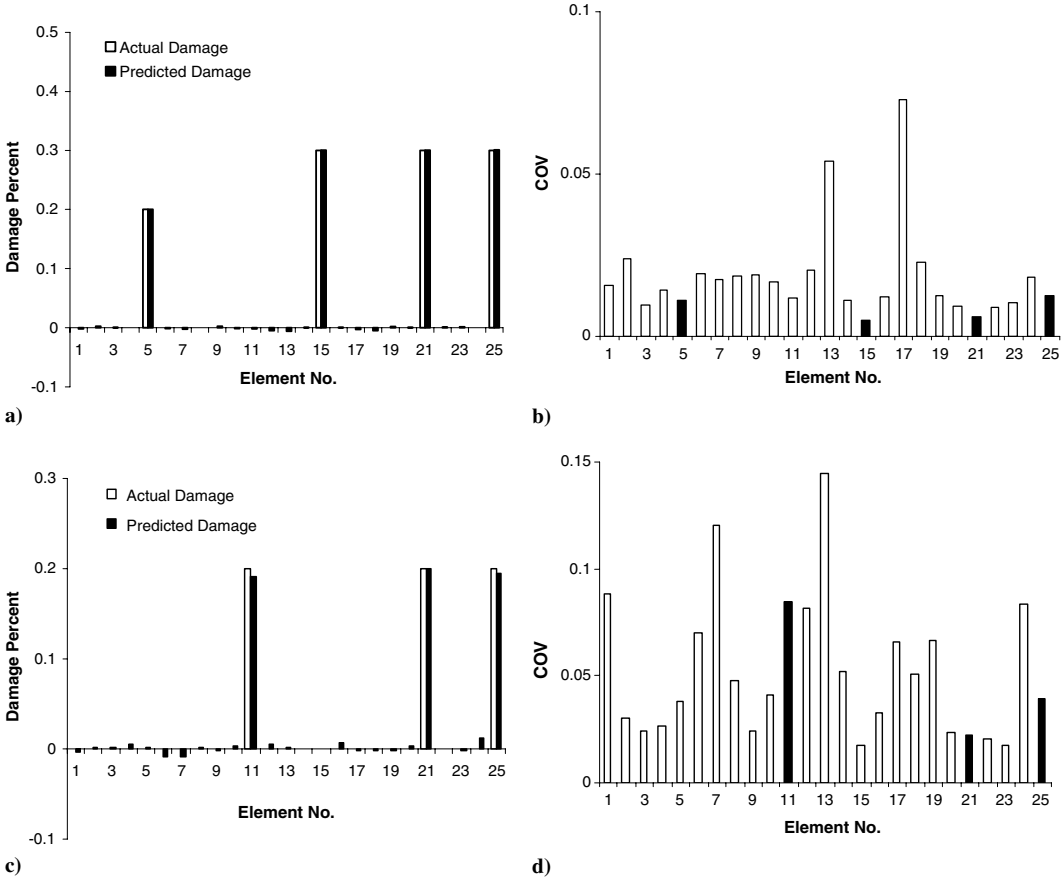

Fig. 12 a) Predicted truss stiffness change for case 6, b) COV of predicted stiffness parameters, c) predicted truss stiffness change for case 6, and d) COV of predicted stiffness parameters.

Table 3 Selected frequency ranges for frame model updating

Damage case: 1, 2	Damage case: 3, 4	Damage case: 5, 6
60–70	110–120	60–70
105–120	210–220	105–120
205–215	255–270	205–215
25026–5	290–310	250–265
290–310	440–455	290–310
——	——	440–455

Table 4 Frequency ranges for model updating of frame with distributed damage

Damage case: tapered beam	Damage case: deterioration
60–73	185–188
84–88	202–210
97–100	245–250
115–150	220–230
200–210	260–268
190–195	283–290
233–238	410–415

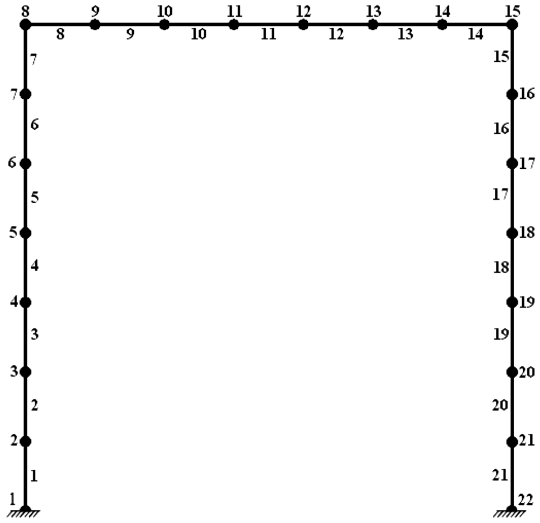

Fig. 13 Two-dimensional frame structure.

Figures 14–17 show that this method is capable of detecting changes of stiffness and mass parameters, while Figs. 18 and 19 show ability to detect mass and stiffness parameters simultaneously. Attention to Figs. 16 and 17 (mass detection cases) shows that, although COV of the predicted parameters is very low, elements adjusted at the corner (element numbers 7, 8, 14 and 15) do not have a COV as low as other elements. Noting that element numbers 1 and 21 are removed from model updating, this means that the mass of these elements has a small continuation to the response and sensitivity equations of the structure in comparison to the mass of the other elements. The norm of the sensitivity matrix for corresponding columns for these elements was low in comparison to other elements, which proves that these elements contribute less to the sensitivity matrix.

Figures 18 and 19 show that the proposed method is capable of simultaneously estimating mass and stiffness parameters at the element level. As stated earlier, ignoring the axial parameters is theoretically a source of error; however, successful results of this example using simulated noisy data proved that participation of axial parameters in the presence of bending behaviors is small and can be ignored.

To further investigate the robustness of the proposed method for parameter estimation, the frame example shown in Fig. 13 is modified. The same frame is investigated using a tapered beam and two tapered columns. Initial bending rigidity values of elements 7, 8, 14, and 15 are increased to 1.7 of the original bending rigidities (EI) and initial bending rigidity values of the elements 6, 9, 13, and 16 are increased to 1.25. The frequency set in the first column of Table 4 is selected for model updating. For this example, the predicted parameters EI and related COV are shown in Fig. 20. As this figure indicates, this method is capable of detecting damage of a frame with variable bending rigidities with low COVs.

Also, damage is not always localized and might appear as deterioration of all structural elements. To investigate the ability of the proposed method in such a case, and as a damage case, bending rigidities of all elements of the frame shown in Fig. 13 are contaminated with 20-percent random damage. The frequency set in the second column of Table 4 is used for model updating. Figure 21 shows the estimated parameters and COV of the predicted parameters. Similar to all other examples, the distributed damage is successfully estimated with very low coefficients of variation.

The authors have performed several other beam, frame, and truss examples in the presence of measurement errors. They all demonstrated robustness of the proposed method with successful parameter estimations and low COVs.

In summary, this study showed that using the proposed approximations of the transfer function yields a quasi-linear sensitivity equation and a robust model updating method even in the presence of high levels of noise. Matching the norms of the exact sensitivity equation with the one proposed here allows one to select the best frequency points for model updating. The results of this study also show that selecting the frequency points based on the sensitivity value increases the robustness of the parameter estimation method.

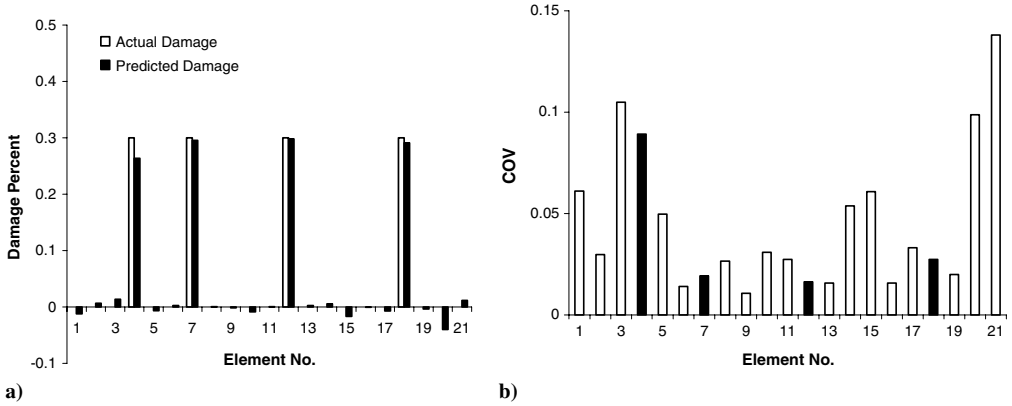

a) b)

Fig. 14 a) Actual and predicted frame stiffness change for case 1 and b) COV of predicted parameters.

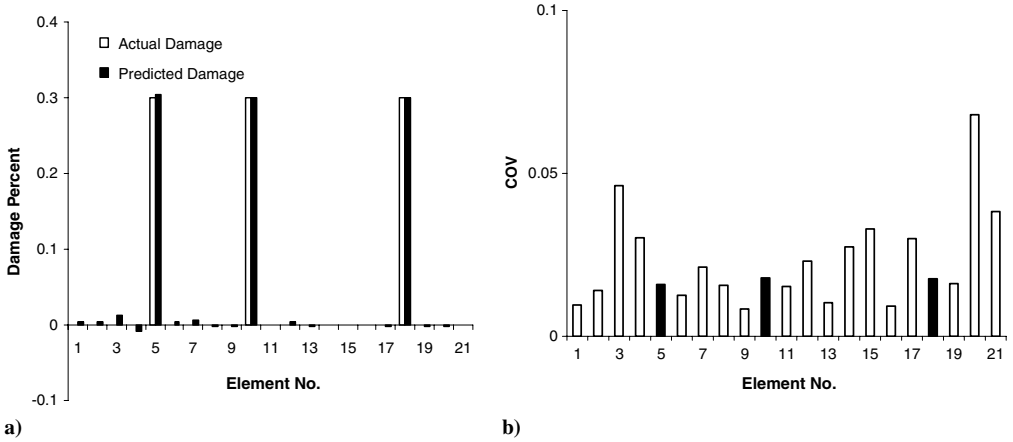

Fig. 15 a) Actual and predicted frame stiffness change for case 2 and b) COV of predicted parameters.

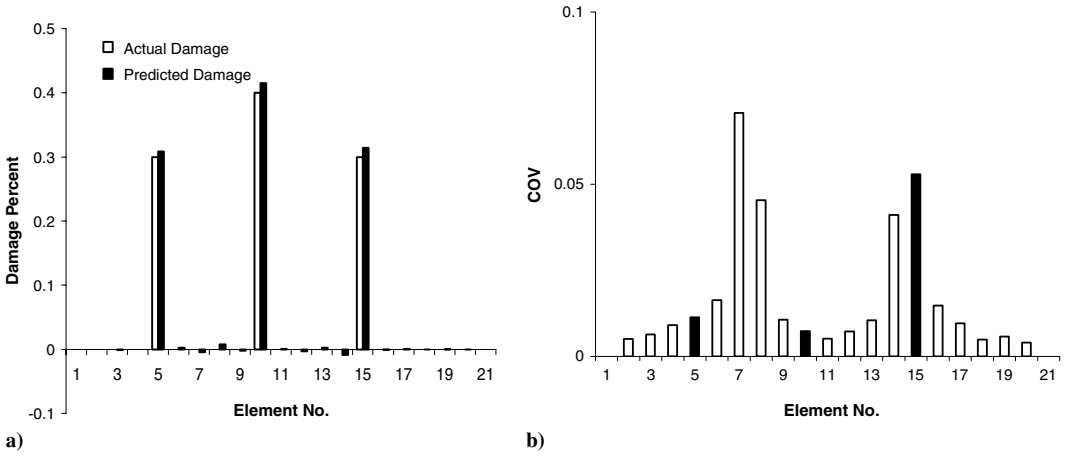

Fig. 16 a) Actual and predicted frame mass change for case 3 and b) COV of predicted parameters.

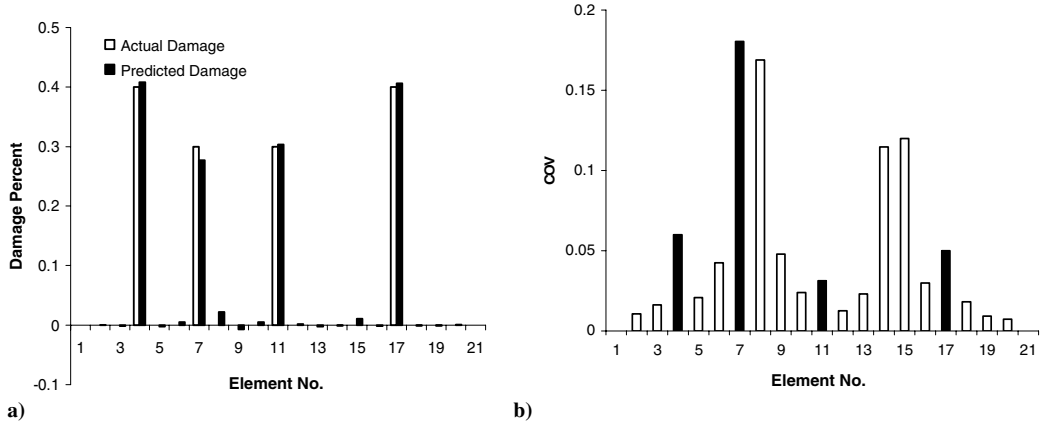

Fig. 17 a) Actual and predicted frame mass change for case 4 and b) COV of predicted parameters.

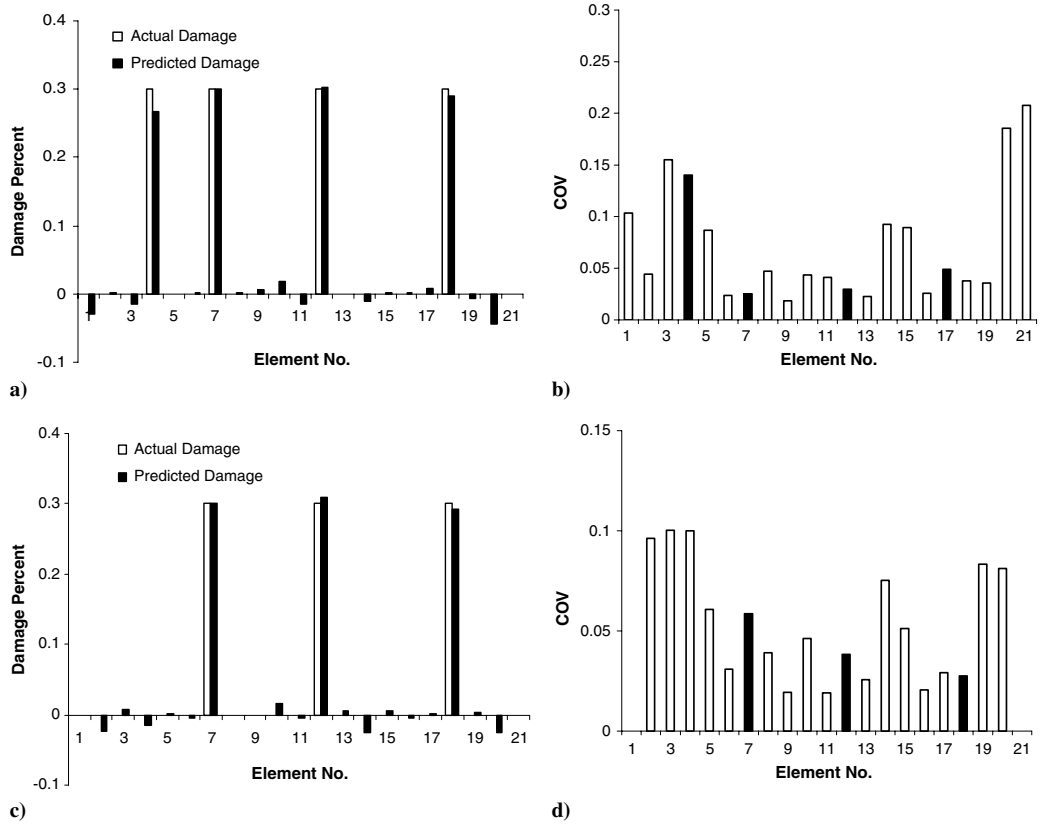

Fig. 18 a) Predicted frame stiffness change for case 5, b) COV of predicted stiffness parameters, c) predicted frame mass change for case 5, and d) COV of predicted mass parameters.

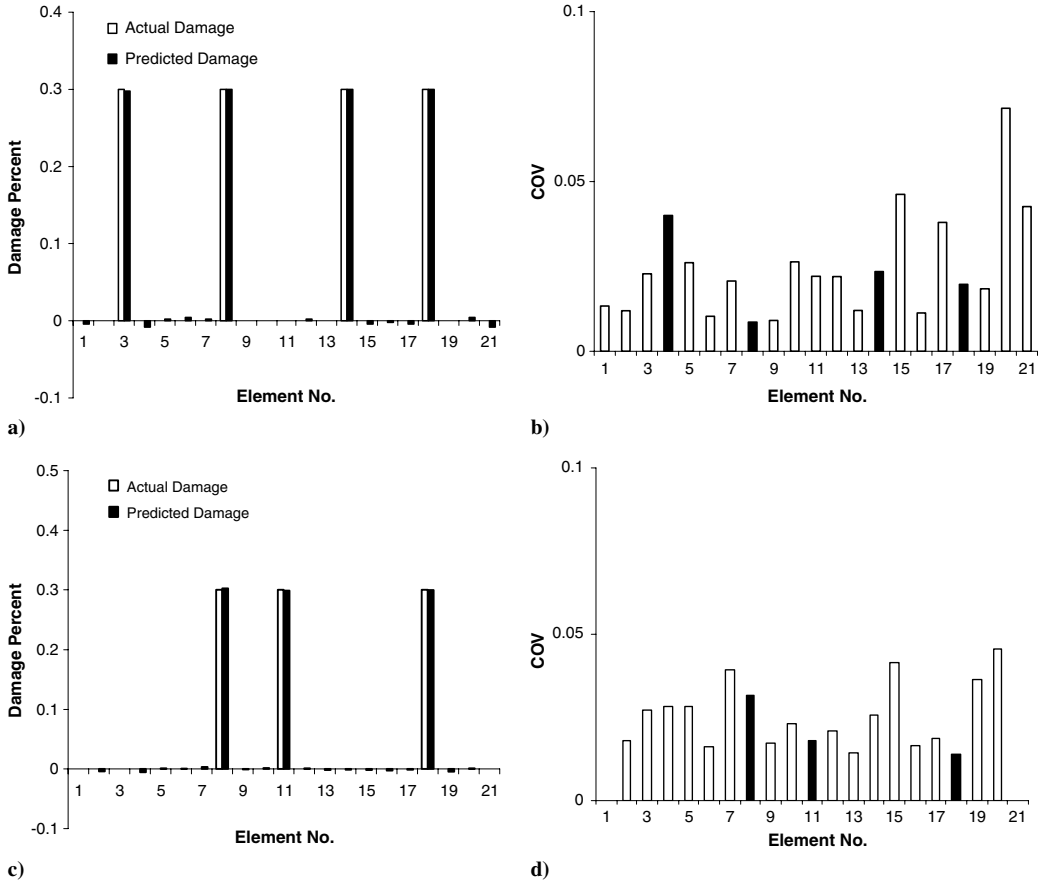

Fig. 19 a) Predicted frame stiffness change for case 6, b) COV of predicted stiffness parameters, c) predicted frame mass change for case 6, and d) COV of predicted mass parameters.

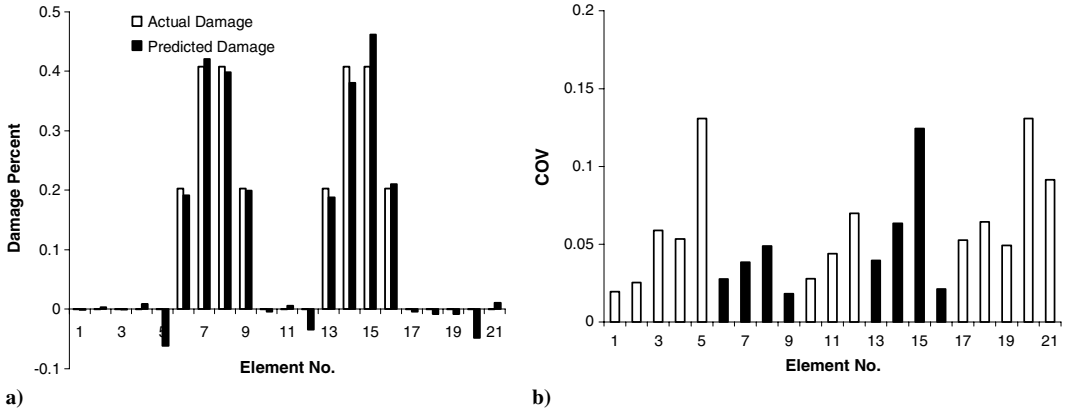

Fig. 20 a) Actual and predicted frame stiffness for tapered beam and b) COV of predicted parameters.

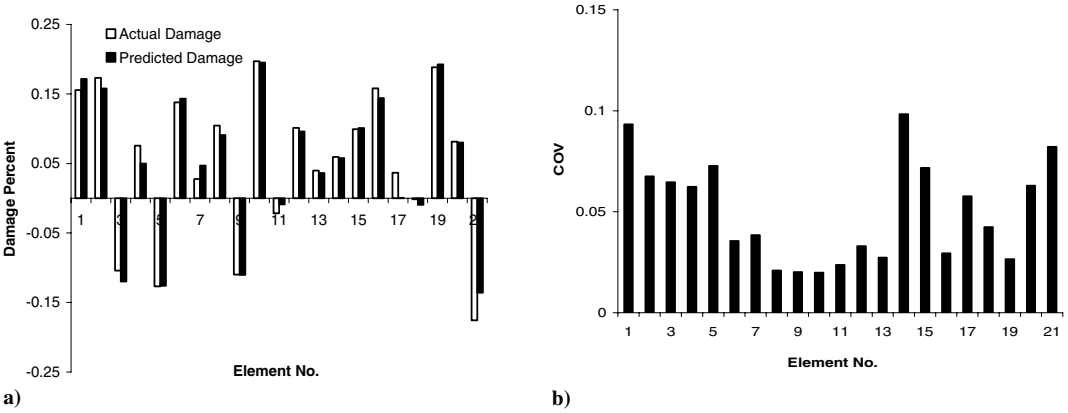

Fig. 21 a) Actual and predicted parameters for deterioration case and b) COV of predicted parameters.

VII. Conclusions

In this paper, frequency response spectrums of measured strains are used for simultaneous stiffness and mass parameter estimation at the element level. Parameter estimates are used for finite element model updating and damage detection of structures. Element level sensitivity equations of the FRF are derived as a function of the stiffness, mass, and damping changes. Measured natural frequency of damaged structures and the mode shapes of intact structures are used to develop a well-approximated evaluation of the transfer function of the damaged structure. The overall formulation yields a quasi-linear sensitivity equation for parameter estimation that improves the stability and robustness of the method against measurement errors. To decrease the effects of noisy measurements, excitation frequency points for model updating are selected based on the second norm of the sensitivity matrix and the best region of frequency points are addressed to avoid nonsmooth behavior of the optimization process. Sensitivity equations are weighted by their second norm to improve the quality of parameter estimation. The proposed method was successfully applied to a truss and a frame using simulated noisy strain data for identification of mass and stiffness parameters, both individually and simultaneously.

References

[1] Salawu, O. S., "Detection of Structural Damage Through Changes in Frequency: A Review," *Engineering Structures*, Vol. 19, No. 9, 1997, pp. 718–723. doi:10.1016/S0141-0296(96)00149-6

[2] Sohn, H., Farrar, C. R., Hemez, F. M., Shunk, D. D., Stinemates, D. W., and Nadler, B. R., "A Review of Structural Health Monitoring Literature: 1996–2001," Los Alamos National Lab. Rept. LA-13976-MS, 2003.

[3] Pandey, A. K., Biswas, M., and Samman, M. M., "Damage Detection from Changes in Curvature Mode Shapes," *Journal of Sound and Vibration*, Vol. 145, No. 2, 1991, pp. 321–332. doi:10.1016/0022-460X(91)90595-B

[4] Ratcliffe, C. P., "Damage Detection Using a Modified Laplacian Operator on Mode Shape Data," *Journal of Sound and Vibration*, Vol. 204, No. 3, 1997, pp. 505–517. doi:10.1006/jsvi.1997.0961

[5] Sanayei, M., and Saletnik, M. J. G., "Parameter Estimation of Structures from Static Strain Measurements, 1: Formulation," *Journal of Structural Engineering*, Vol. 122, No. 5, 1996, pp. 555–562. doi:10.1061/(ASCE)0733-9445(1996)122:5(555)

[6] Sanayei, M., Imbaro, G. R., McClain, J. A. S., and Brown, L. C., "Structural Model Updating Using Experimental Static Measurements," *Journal of Structural Engineering*, Vol. 123, No. 6, 1997, pp. 792–798. doi:10.1061/(ASCE)0733-9445(1997)123:6(792)

[7] Liu, P. L., "Parametric Identification of Plane Frames Using Static Strain," *Proceedings of the Royal Society of London*, 1996, pp. 29–45, 452.

[8] Liu, P. L., and Chian, C. C., "Parametric Identification of Truss Structures Using Static Strains," *Journal of Structural Engineering*, Vol. 123, No. 7, 1997, pp. 927–933. doi:10.1061/(ASCE)0733-9445(1997)123:7(927)

[9] Shenton, H. W., and Xiaofeng, H., "Damage Identification Based on Dead Load Redistribution: Methodology," *Journal of Structural Engineering*, Vol. 132, No. 8, 2006, pp. 1254–1263. doi:10.1061/(ASCE)0733-9445(2006)132:8(1254)

[10] Pabst, U., and Hagedorn, P., "On the Identification of Localized Losses of Stiffness in Structures," *ASME 1993 Design Engineering Technical Conference (DE59)*, Vol. 59, American Society of Mechanical Engineers, Design Engineering Div., New York, 1993, pp. 99–104.

[11] Salawu, O. S., and Williams, C., "Damage Location Using Vibration Mode Shapes," *Proceedings of the 12th International Modal Analysis Conference*, Honolulu, HI, Feb. 1994, pp. 933–9.

[12] Stubbs, N., and Kim, J. T., "Damage Localization Without Baseline Modal Parameter," *AIAA Journal*, Vol. 34, No. 8, 1996, pp. 1644–9.

[13] Wahab, M. M. A., Roeck, G. D., and Peeters, B., "Parameterization of Damage in Reinforced Concrete Structures Using Modal Updating,"

Journal of Sound and Vibration, Vol. 228, No. 4, 1999, pp. 717–730. doi:10.1006/jsvi.1999.2448

[14] Shi, Z. Y., Law, S. S., and Zhang, L. M., "Structural Damage Detection from Modal Strain Energy Change," *Journal of Engineering Mechanics*, Vol. 126, No. 12, 2000, pp. 1216–1223. doi:10.1061/(ASCE)0733-9399(2000)126:12(1216)

[15] Lestari, W., and Qiao, P., "Damage Detection of Fiber-Reinforced Polymer Honeycomb Sandwich Beams," *Composite Structures*, Vol. 67, No. 3, 2005, pp. 365–373. doi:10.1016/j.compstruct.2004.01.023

[16] Lew, J. S., "Using Transfer Function Parameter Changes for Damage Detection of Structures," *AIAA Journal*, Vol. 33, No. 11, 1995, pp. 2189–2193. doi:10.2514/3.12965

[17] Wang, Z., Lin, R. M., and Lim, M. K., "Structural Damage Detection Using Measured FRF Data," *Computer Methods in Applied Mechanics and Engineering*, Vol. 147, No. 1, 1997, pp. 187–197. doi:10.1016/S0045-7825(97)00013-3

[18] Lee, D. H., and Hwang, W. S., "Parametric Optimization of Complex Systems Using a Multi-Domain FRF-Based Sub Structuring Method," *Computers and Structures*, Vol. 81, Nos. 22–23, 2003, pp. 2249–2257. doi:10.1016/S0045-7949(03)00288-8

[19] Keilers, C. H. Jr., and Chang, F. K., "Identifying Delamination in Composite Beams Using Built-In Piezoelectrics, Part 1: Experiments and Analysis," *Journal of Intelligent Material Systems and Structures*, Vol. 6, No. 5, 1995, pp. 649–663. doi:10.1177/1045389X9500600506

[20] Sampaio, R. P. C., Maia, N. M. M., and Silva, J. M. M., "Damage Detection Using the Frequency-Response-Function Curvature Method," *Journal of Sound and Vibration*, Vol. 226, No. 5, 1999, pp. 1029–1042. doi:10.1006/jsvi.1999.2340

[21] Schulz, M. J., Pai, P. F., and Inman, D. J., "Health Monitoring and Active Control of Composite Structures Using Piezoceramic Patches," *Composites, Part B: Engineering*, Vol. 30, No. 7, 1999, pp. 713–25.

[22] Colin, P., and Ratcliffe, C. P., "A Frequency and Curvature Based Experimental Method for Locating Damage in Structures," *Transactions of the ASME*, Vol. 122, No. 3, 2000, pp. 324–329. doi:10.1115/1.1303121

[23] Sanayei, M., McClain, J. A. S., Wadia-Fascetti, S., and Santini, E. M., "Parameter Estimation Incorporating Modal Data and Boundary Conditions," *Journal of Structural Engineering*, Vol. 125, No. 9, 1999, pp. 1048–1055. doi:10.1061/(ASCE)0733-9445(1999)125:9(1048)

[24] Rahai, A., Bakhtiari-Nejad, F., and Esfandiari, A., "Damage Assessment of Structure Using Incomplete Measured Mode Shapes," *Structural Control and Health Monitoring*, Vol. 14, No. 5, 2007, pp. 808–829. doi:10.1002/stc.183

[25] Park, N. G., and Park, Y. S., "Damage Detection Using Spatially Incomplete Frequency Response Function," *Mechanical Systems and Signal Processing*, Vol. 17, No. 3, 2003, pp. 519–532. doi:10.1006/mssp.2001.1423

[26] Sazonov, E., and Klinkhachorn, P., "Optimal Spatial Sampling Interval for Damage Detection by Curvature or Strain Energy Mode Shapes," *Journal of Sound and Vibration*, Vol. 285, Nos. 4–5, 2005, pp. 783–801. doi:10.1016/j.jsv.2004.08.021

[27] Peterson, L. D., Doebling, S. W., and Alvin, K. F., "Experimental Determination of Local Structural Stiffness by Disassembly of Measured Flexibility Matrices," *Proceedings of 36th AIAA/ASME/ASCE/AHS/ASC Structures, Structural Dynamics, and Materials Conference*, AIAA Paper 95-1090-CP, 1995, pp. 2756–2766.

[28] Ren, Y., and Beards, C. F., "Identification of Joint Properties of a Structure Using FRF Data," *Journal of Sound and Vibration*, Vol. 186, No. 4, 1995, pp. 567–587. doi:10.1006/jsvi.1995.0469

[29] Ren, W. X., De Roeck, G., "Structural Damage Identification Using Modal Data 1: Simulation Verification," *Journal of Structural Engineering*, Vol. 128, No. 1, 2002, pp. 87–95. doi:10.1061/(ASCE)0733-9445(2002)128:1(87)

[30] Lin, R. M., Lim, M. K., and Ong, J. H., "Improving Finite Element Models in the Higher Frequency Range Using Modified Frequency Response Function Sensitivity Method," *Finite Elements in Analysis and Design*, Vol. 15, No. 2, 1993, pp. 157–175. doi:10.1016/0168-874X(93)90063-V

J. Wei
Associate Editor